Athermal Photonic Crystal Membrane Reflectors on Diamond

Shihchia Liu, Deyin Zhao, Jung-Hun Seo, Yonghao Liu, Zhenqiang Ma, *Senior Member, IEEE*, and Weidong Zhou, *Senior Member, IEEE*

***Abstract*— We report here experimental demonstration of Fano resonance photonic crystal Si membrane reflectors on diamond for much improved thermal performance. At normal incidence, high reflection is obtained over a broad spectral band, with reflectivity greater than 95% from 1260 to 1450 nm. The measured reflection spectrum agrees well with the theoretical design. The improved thermal performance, with much reduced temperature rise, was also observed experimentally over a wide range of high incident optical power intensities. Such athermal Si membrane reflectors on diamond offer great opportunities for the applications in energy efficient lasers and high-power lasers.**

***Index Terms*— Photonic crystals reflector, high thermal conductivity, printing transfer.**

I. Introduction

OVER the past decades, rapid and significant progresses have been made in dielectric membrane reflectors (MRs) based on Fano resonance, or guided resonances, with high refractive index contrast structures including one-dimensional (1D) grating [1]–[5] and two-dimensional (2D) photonic crystal slabs (PCS) [6]–[11]. These single layer membrane reflectors have also been successfully incorporated into VCSELs, with the demonstrations of ultra-compact VCSELs on III-V and on Silicon substrates [8], [11]. To achieve both broad bandwidth and high reflectivity, higher refractive index contrast (Δn) between the patterned membrane reflector layer and its surrounding medium (above and below) is needed [12], [13]. And most membrane reflectors demonstrated so far have either suspended configurations (with air above and below) or surrounded with low index (e.g. glass substrate with n$\sim$1.45). However these low index buffer materials (air or glass) have very small thermal conductivity ($\sim$1 W$\cdot$m$^{-1}\cdot$K^{-1}), which results in very poor thermal performances for heat dissipation from the laser cavity.

Thermal engineering of the cavity to enable excellent heat dissipation from the active region and to minimize the temperature rise of the lasing cavity is of great importance towards ultra-compact uncooled lasers operating over wide temperature ranges, and high power lasers with simplified thermal mechanical designs.

As in [14], the authors reported up to 43 °C continuous-wave lasing from a double Si/SiO_2 PCS VCSEL, with heat flowing laterally following the III-V active layers. Athermal integrated photonic circuits and dramatically improved thermal management in microlasers can also be obtained via the use of diamond/AlN buffer/substrate layers. Heat can dissipate more effectively from the cavity through these buffer/substrate layers, which have excellent thermal conductivities (diamond: 1,900 W m^{-1}K^{-1}, AlN: 280 W m^{-1}K^{-1}) than air or glass (SiO_2). However diamond and AlN also have relatively higher refractive indexes (n $\sim$ 2.35) at near infrared band, which presents a design challenge for the membrane reflectors.

As in [15], a Si based 1D high contrast grating (HCG) on diamond reflector was proposed and used as top and bottom mirrors into high power vertical external cavity surface emitting laser (VECSEL) cavity designs. For this proposed HCG reflector design, the high reflection can be only obtained for the incident light from the substrate to air due to higher index contrast at Si (n$\sim$3.48) and air (n=1) interface. On the contrary incident direction, the reflection is much lower. This Si HCG on diamond structure (Δn$\sim$1.13) is similar as the surface grating, [16], [17] where the grating material is same as the substrate (Δn=0). For all of these sub-wavelength gratings, including the HCGs on the low index substrates (Δn$\sim$2.48), all higher order diffraction modes are evanescent except the zeroth-order mode at the interface with high index contrast, which attributes to the high reflection [5], [16], [18].

In this letter, we report detailed design and first experimental demonstration of reflection and thermal properties in 2D PCS based Si membrane reflectors (Si-MRs) on diamond substrate at 1,500 nm near-infrared wavelength range. Shown in Fig. 1(a) is the sketch of the designed Si-MR on diamond substrate, which consists of a 2D square lattice photonic crystal structure with period $a = 860$ nm and air hole radius $r = 0.45a$. The Si membrane thickness t is 340 nm. The corresponding reflection spectrum is simulated by using the Fourier Modal Method with Stanford Stratified Structure Solver (S4) software package [19] and plotted in Fig. 1(b).

Manuscript received December 2, 2014; revised February 12, 2015; accepted February 23, 2015. Date of publication February 26, 2015; date of current version April 24, 2015. This work was supported in part by the U.S. Army Research Office under Contract W911NF-09-1-0505, in part by the U.S. National Science Foundation through the Division of Electrical, Communications and Cyber Systems under Grant ECCS-1308520, and in part by the Air Force Office of Scientific Research, Arlington, VA, USA, under Contract FA9550-11-C-0026.

S. Liu, D. Zhao, Y. Liu, and W. Zhou are with the NanoFAB Center, Department of Electrical Engineering, University of Texas at Arlington, Arlington, TX 76019 USA (e-mail: shih-chia.liu@mavs.uta.edu; dzhao@uta.edu; yonghao.liu@mavs.uta.edu; wzhou@uta.edu).

J.-H. Seo and Z. Ma are with the Department of Electrical and Computer Engineering, University of Wisconsin—Madison, Madison, WI 53706 USA (e-mail: seo8@wisc.edu; mazq@engr.wisc.edu).

Color versions of one or more of the figures in this letter are available online at http://ieeexplore.ieee.org.

Digital Object Identifier 10.1109/LPT.2015.2407394

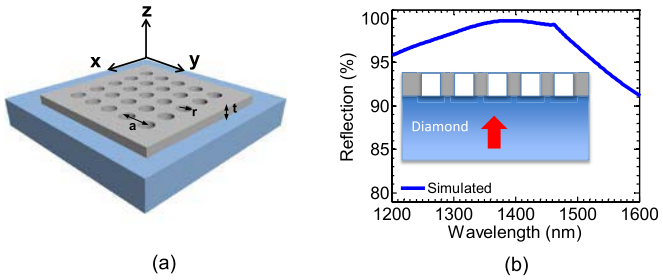

Fig. 1. (Color Online) (a) 3D sketch of a 2D square lattice PC Si-MR structure on a diamond substrate; and (b) simulated reflection for the designed Si-MR on diamond substrate with incidence from the substrate side.

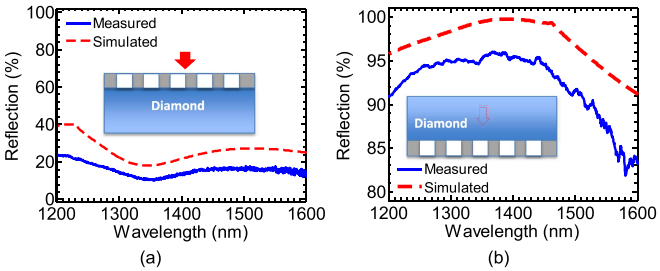

Fig. 3. (Color Online) Measured (solid blue line) and simulated (dashed red line) reflection spectra for Si-MR on diamond: (a) with incidence from top Si-MR side; and (b) with incidence from the diamond substrate side.

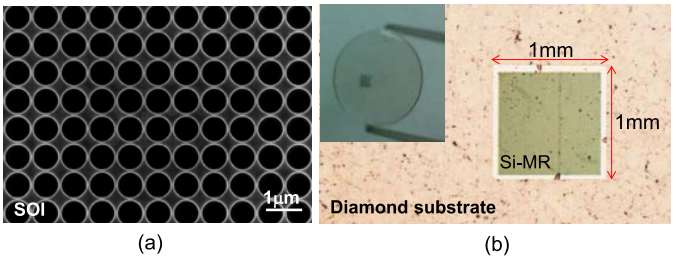

Fig. 2. (Color Online) (a) A scanning electron microscope (SEM) top-view image of the PC structure patterned on SOI. (b) Optical microscopic images of Si-MR reflector transferred on diamond substrate, with the inset shown the complete view of Si-MR on diamond substrate.

The inset in Fig. 1(b) shows the direction of incident light from the diamond substrate. According to this set of Si-MR design, one can expected to get a broad reflection band from 1,350 nm to 1,470 nm with reflectivity greater than 99%, or an even broader bandwidth from 1,250 nm to 1,500 nm with reflectivity greater than 96%.

II. Si Nanomembrane Transfer on Diamond Substrate

A Si-MR with 1 × 1mm^2 pattern area was first fabricated on SOI (340 nm top Si and 1 μm BOX) based on standard e-beam lithography patterning technique and dry-etching processes. Fig. 2(a) shows the scanning electron microscope (SEM) top-view image of the Si-MR on SOI. The patterned Si-MR was first released from the SOI substrate and then transferred onto the diamond substrate, based on PDMS printing transfer technique reported earlier [20]. The transfer printing process starts with the release of the patterned Si-MR, by immersing the patterned SOI structure in buffered hydrofluoric acid (HF) solution to remove the BOX layer. A PDMS stamp, with optimized adhesion force, is used to pick up the released/detached patterned Si-MR. With PDMS stamp as the transfer media, patterned Si-MR structure is then printed to the foreign diamond substrate. Special care is taken on the adhesion force of PDMS stamp and the NM picking-up and printing (peeling-off PDMS) speeds [20].

Fig. 2(b) displays the optical microscope images of the transferred Si-MR on diamond. The inset shows the overview image of the sample with the Si-MR in the center. The quality of the transferred Si-MR is pretty good although the surface of the diamond substrate is a little rough with some black dots. These black dots come from the diamond surface itself, which can be seen outside Si-MR region in Fig. 2(b). The diamond substrate we used here is one kind of optical grade polycrystalline CVD diamond (Element Six Corp) with the size of 8 mm round, the thickness of 0.5 mm, the surface roughness >30 nm and the thermal conductivity is around 1900 W m^{-1} K^{-1}. To obtain a high quality surface, the substrate surface was carefully cleaned by a mixture of $HNO_3/H_2SO_4/NaNO_3$, followed by a deionized (DI) water rinse before the Si-MR was transferred on it.

III. MR Reflector Characteristics

Shown in Fig. 3(a) and (b) are the measured and simulated reflection spectra of Si-MR with incident light from the top Si-MR air side and the diamond substrate side, respectively. The reflections are measured at surface normal incidence using white light source. The reflection from the top Si-MR side was directly measured by shinning the light from the air to Si-MR. The reflectivity was obtained by normalizing with the reflection spectrum measured from the calibrated gold reference mirror (Edmund Optics) with measured reflectivity of 97.8% over a spectral range of 1200 -1600 nm. In order to measure the reflection of Si-MR from diamond substrate side, we measured the transmission (T) spectrum with the incident light from diamond substrate side. The reflection (R) is obtained by using equation R = 1-T, assuming absorption is zero (both silicon and diamond are transparent around 1,550 nm). Due to the presence of the diamond substrate and its rough surface, the reflection beam are divergent through the diamond substrate and thus the corresponding reflection spectrum directly measured from the diamond substrate side is not accurate. Based on the results shown in Fig. 3, we can see the measured and the simulated reflections match very well. The reflection from the substrate is close to 95% over 150 nm wavelength range from 1,300 nm to 1,450 nm. The estimated reflection measurement error is around 1-2%, which is mainly associated with the scattering losses on the rough surface, and the focused non-collimated incident beam, which results in non-ideal surface-normal incidence. The reflection performance can be further improved by using polished diamond substrate with much small surface roughness to improve the transfer quality or single crystalline diamond substrate to reduce inner light scattering.

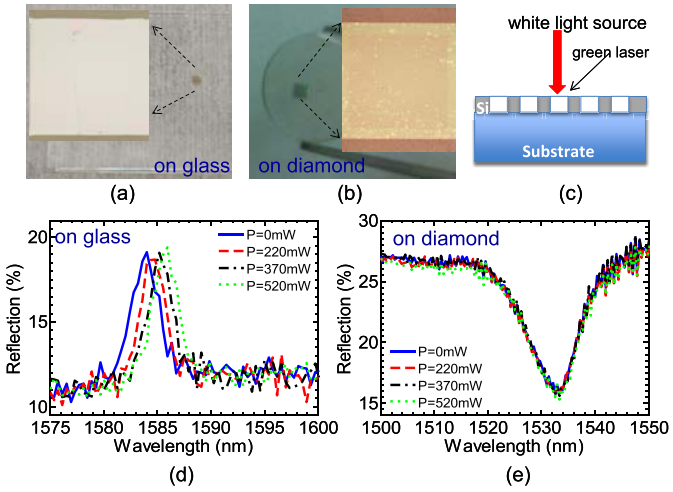

Fig. 4. (Color Online) Micrograph images of transferred silicon nanomembrane (Si-NM) Fano filters (a) on glass, (b) on diamond substrate. The insets are the zoom-in images. (c) Sketch of the reflection test with high power green laser shining from the side for heating the Si-NM Fano filter. Measured reflection spectra of the filters under different laser power heat levels for Si Fano filters (d) on glass substrate and (e) on diamond substrate.

Finally, structural thermal performance was investigated. Since the Si-MR structure considered here may be incorporated into laser cavity design, we consider spectral shift associated with temperature rise in Si-MR, as a result of high incident optical power intensities. In order to precisely measure the spectral shift, we prepared narrow band high Q Fano filters. Two Fano filters with similar parameters were transferred onto glass and diamond substrate, respectively [21]. Fig. 4(a) and (b) show the images of the transferred high Q filters on glass and diamond substrate, respectively, where the insets show their zoom-in images. The sketch of the testing condition is shown in Fig. 4(c). High power green laser (spot diameter around 3∼4 mm) was used as the pump source to heat up the Si high Q filters (1 mm × 1 mm) and shine it for 10 minutes to stabilize temperature prior to measurement. Surface-normal white light source (with low incident optical power) is used to measure the reflection spectrum, with continuous wave green pump laser incident on the Si-MR simultaneously.

With the increase in green laser power, the reflection peak of the filter on glass shifts around 2 nm to longer wavelength as shown in Fig. 4(d), while the reflection dip of the filter on diamond does not shift under the same condition as shown in Fig. 4(e). It is known that both symmetric Lorentzian and asymmetric Fano line shapes can evolve with the control of temporal-phase delay, which results in single peak or dip symmetric lineshapes and asymmetric peak/dip or dip/peak lineshapes [22], [23]. We observed both theoretically and experimentally all these four types of resonance lineshapes, including two filters shown in Fig. 4, where both filters have similar lattice parameters on different substrates. Differences in the refractive index between the glass and the diamond substrates, result in the phase change of Fano resonance. Based on the simulations, if the filter on glass has a 2 nm peak shift, the refractive index of Si will change around 4.5×10^{-3} due to thermo-optic effect. According to the

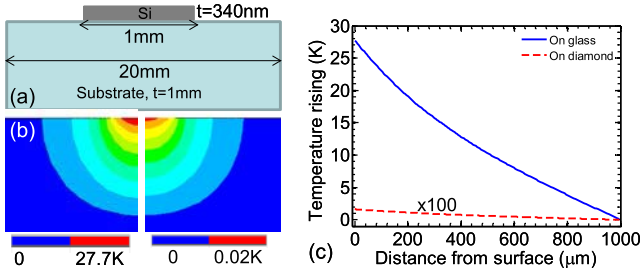

Fig. 5. (Color online) (a) A sketch of the Si filter on a substrate used for the thermal simulation; (b) thermal field distributions of the filters on glass (left) and diamond (right); (c) temperature rise as a function of position along the vertical direction from the device surface to the bottom substrate.

thermo-optic coefficients of Si ($dn/dT = 1.86 \times 10^{-4}$/K) [24] and glass ($dn/dT = 1.0 \times 10^{-5}$/K) [25], the estimated temperature rise inside Si-MR on glass is around 24 K. Based on the structural parameters of these samples and Si absorption at 532nm, the thermal simulation was carried out using ANSYS. Fig. 5(a) shows the device structure sketch used in the thermal simulation. The temperature rise (ΔT) distributions inside the filter on glass and on diamond are shown in the left and the right panels of Fig. 5(b). The temperature rises (ΔT) along the vertical direction from the surface of Si-MR to the bottom substrate is also plotted in Fig. 5(c), where their maximum temperature rises (ΔT) are around 27.7K and 0.02K, for the structure on glass and on diamond substrate, respectively. One can see the thermal simulation results match well with above estimated temperature rises as well.

IV. Conclusion

In conclusion, we demonstrated 2D photonic crystal Si-MR on diamond with measured 95% reflection over 150 nm spectral bandwidth at wavelength around 1,500 nm. Very good athermal performance property with fast heat dissipation was confirmed based on the experimental and theoretical analysis. All the experimental results agree well with the theoretical designs. Therefore it is completely feasible to get close to 100% reflection of such thermally engineered Si-MR by further improving the diamond surface and the transfer quality. Such kind of thermally engineered mirrors will be the good candidates to develop athermal photonics integrated circuits and mircrolasers. And it is highly desirable for the incorporation of such MR structures into energy efficient lasers [11] and high power lasers [15].

References

[1] C. F. R. Mateus, M. C. Y. Huang, L. Chen, C. J. Chang-Hasnain, and Y. Suzuki, "Broad-band mirror (1.12–1.62 μm) using single-layer sub-wavelength grating," *IEEE Photon. Technol. Lett.*, vol. 16, no. 7, pp. 1676–1678, Jul. 2004.

[2] S. Boutami, B. Ben Bakir, P. Regreny, J. L. Leclercq, and P. Viktorovitch, "Compact 1.55 μm room-temperature optically pumped VCSEL using photonic crystal mirror," *Electron. Lett.*, vol. 43, no. 5, pp. 37–38, Mar. 2007.

[3] M. C. Y. Huang, Y. Zhou, and C. J. Chang-Hasnain, "A surface-emitting laser incorporating a high-index-contrast subwavelength grating," *Nature Photon.*, vol. 1, pp. 119–122, Apr. 2007.

[4] Y. Ding and R. Magnusson, "Resonant leaky-mode spectral-band engineering and device applications," *Opt. Exp.*, vol. 12, no. 23, pp. 5661–5674, 2004.
[5] R. Magnusson and M. Shokooh-Saremi, "Physical basis for wideband resonant reflectors," *Opt. Exp.*, vol. 16, no. 5, pp. 3456–3462, 2008.
[6] V. Lousse, W. Suh, O. Kilic, S. Kim, O. Solgaard, and S. Fan, "Angular and polarization properties of a photonic crystal slab mirror," *Opt. Exp.*, vol. 12, no. 8, pp. 1575–1582, 2004.
[7] S. Boutami *et al.*, "Broadband and compact 2-D photonic crystal reflectors with controllable polarization dependence," *IEEE Photon. Technol. Lett.*, vol. 18, no. 7, pp. 835–837, Apr. 1, 2006.
[8] C. Sciancalepore *et al.*, "CMOS-compatible ultra-compact 1.55-μm emitting VCSELs using double photonic crystal mirrors," *IEEE Photon. Technol. Lett.*, vol. 24, no. 6, pp. 455–457, Mar. 15, 2012.
[9] H. Yang *et al.*, "Resonance control of membrane reflectors with effective index engineering," *Appl. Phys. Lett.*, vol. 95, no. 2, p. 023110, 2009.
[10] D. Zhao, H. Yang, S. Chuwongin, J. H. Seo, Z. Ma, and W. Zhou, "Design of photonic crystal membrane-reflector-based VCSELs," *IEEE Photon. J.*, vol. 4, no. 6, pp. 2169–2175, Dec. 2012.
[11] H. Yang *et al.*, "Transfer-printed stacked nanomembrane lasers on silicon," *Nature Photon.*, vol. 6, pp. 615–620, Jul. 2012.
[12] C. F. R. Mateus, M. C. Y. Huang, Y. Deng, A. R. Neureuther, and C. J. Chang-Hasnain, "Ultrabroadband mirror using low-index cladded subwavelength grating," *IEEE Photon. Technol. Lett.*, vol. 16, no. 2, pp. 518–520, Feb. 2004.
[13] T. Sang, L. Wang, S. Ji, Y. Ji, H. Chen, and Z. Wang, "Systematic study of the mirror effect in a poly-Si subwavelength periodic membrane," *J. Opt. Soc. Amer. A*, vol. 26, no. 3, pp. 559–565, 2009.
[14] C. Sciancalepore *et al.*, "Thermal, modal, and polarization features of double photonic crystal vertical-cavity surface-emitting lasers," *IEEE Photon. J.*, vol. 4, no. 2, pp. 399–410, Apr. 2012.
[15] V. Iakovlev *et al.*, "Double-diamond high-contrast-gratings vertical external cavity surface emitting laser," *J. Phys. D, Appl. Phys.*, vol. 47, no. 6, p. 065104, 2014.
[16] S. Goeman *et al.*, "First demonstration of highly reflective and highly polarization selective diffraction gratings (GIRO-gratings) for long-wavelength VCSELs," *IEEE Photon. Technol. Lett.*, vol. 10, no. 9, pp. 1205–1207, Sep. 1998.
[17] J. Lee, S. Ahn, H. Chang, J. Kim, Y. Park, and H. Jeon, "Polarization-dependent GaN surface grating reflector for short wavelength applications," *Opt. Exp.*, vol. 17, no. 25, pp. 22535–22542, 2009.
[18] Y. Zhou *et al.*, "High-index-contrast grating (HCG) and its applications in optoelectronic devices," *IEEE J. Sel. Topics Quantum Electron.*, vol. 15, no. 5, pp. 1485–1499, Sep./Oct. 2009.
[19] V. Liu and S. Fan, "S^4: A free electromagnetic solver for layered periodic structures," *Comput. Phys. Commun.*, vol. 183, no. 10, pp. 2233–2244, 2012.
[20] H. Yang *et al.*, "Broadband membrane reflectors on glass," *IEEE Photon. Technol. Lett.*, vol. 24, no. 6, pp. 476–478, Mar. 15, 2012.
[21] H. Yang, H. Pang, Z. Qiang, Z. Ma, and W. Zhou, "Surface-normal Fano filters based on transferred silicon nanomembranes on glass substrates," *Electron. Lett.*, vol. 44, no. 14, pp. 858–859, 2008.
[22] A. E. Miroshnichenko, S. Flach, and Y. S. Kivshar, "Fano resonances in nanoscale structures," *Rev. Modern Phys.*, vol. 82, no. 3, p. 2257, 2010.
[23] C. Ott *et al.*, "Lorentz meets Fano in spectral line shapes: A universal phase and its laser control," *Science*, vol. 340, no. 6133, pp. 716–720, 2013.
[24] G. Cocorullo and I. Rendina, "Thermo-optical modulation at 1.5 μm in silicon etalon," *Electron. Lett.*, vol. 28, no. 1, pp. 83–85, 1992.
[25] J. M. Jewell, "Thermooptic coefficients of some standard reference material glasses," *J. Amer. Ceram. Soc.*, vol. 74, no. 7, pp. 1689–1691, 1991.